

# Excitation Spectra of Structurally Dimerized and Spin-Peierls Chains in a Magnetic Field

Weiqiang Yu and Stephan Haas

*Department of Physics and Astronomy, University of Southern California, Los Angeles, CA 90089-0484*  
(April 26, 2024)

The dynamical spin structure factor and the Raman response are calculated for structurally dimerized and spin-Peierls chains in a magnetic field, using exact diagonalization techniques. In both cases there is a spin liquid phase composed of interacting singlet dimers at small fields  $h < h_{c1}$ , an incommensurate regime ( $h_{c1} < h < h_{c2}$ ) in which the modulation of the triplet excitation spectra adapts to the applied field, and a fully spin polarized phase above an upper critical field  $h_{c2}$ . For structurally dimerized chains, the spin gap closes in the incommensurate phase, whereas spin-Peierls chains remain gapped. In the spin liquid regimes, the dominant feature of the triplet spectra is a one-magnon bound state, separated from a continuum of states at higher energies. There are also indications of a singlet bound state above the one-magnon triplet.

75.10.J,72.15.Nj,78.70.Nx,78.30.-j

## I. INTRODUCTION

In the absence of a magnetic field, structurally dimerized spin chains, such as  $(VO)_2P_2O_7$ <sup>1</sup>, have a magnetic response similar to spin-Peierls chains, such as  $CuGeO_3$ <sup>2,3</sup>. In both cases, there is a one-magnon triplet bound state at energy transfers  $\omega = \Delta_z$ , where  $\Delta_z$  measures the singlet-triplet spin gap, followed by a two-magnon continuum of states with an onset at higher frequencies,  $\omega = 2\Delta_z$ .<sup>4</sup> The one-magnon bound state arises from the confinement of soliton-antisoliton pairs due to an effective attractive potential caused by the lattice dimerization.<sup>5,6</sup> In the case of spin-Peierls chains, there is additional coupling of the spins to the elastic degrees of freedom of the lattice, causing the softening of a phonon mode.<sup>7-9</sup> In contrast, the atomic positions of structurally dimerized chains are completely locked, ruling out a feedback between the spins and the phonons. It is this magneto-elastic feedback in the spin-Peierls compounds, which allows the spin gap to remain open even at large magnetic fields,<sup>10</sup> while in the structurally dimerized chains, the gap closes beyond a critical magnetic field strength,  $h_{c1}$ , due to the deconfinement of the soliton-antisoliton pairs. In both cases the triplet spectra become incommensurate at  $h > h_{c1}$ . However, we will see that for the structurally dimerized chains they are gapless soliton-antisoliton continua, whereas in the spin-Peierls compounds the dominant one-magnon bound state remains gapped, acquiring a modulation which depends on the magnitude of the applied field.<sup>10</sup>

In the adiabatic approximation (suppressing the phonon dynamics), the effective Hamiltonian of antiferromagnetically correlated spins coupled to a crystal lattice is given by,

$$H = J \sum_{r=1}^N (1 + \delta_r) \mathbf{S}_r \cdot \mathbf{S}_{r+1} + \frac{K}{2} \sum_{r=1}^N \delta_r^2, \quad (1)$$

where  $J$  is the Heisenberg exchange constant,  $\delta_r$  are local lattice distortions, and  $K$  is the lattice spring constant. The feedback of the phonons to the spin degrees of freedom is contained in the dependence of  $\delta_r$  on  $K$ . In the absence of a magnetic field,  $\delta_r = \delta(-1)^r$ . The dimerization parameter  $\delta$  is a constant for structurally dimerized chains, whereas  $\delta \propto K^{-3/2}$  for spin-Peierls systems.<sup>7,11,12</sup> The structurally dimerized chain can be viewed as a limiting case of Eq. (1) with a vanishing spring constant ( $K = 0$ ) and a “frozen” (inelastic) lattice modulation, which does not vary with an applied magnetic field. On the contrary, spin-Peierls chains in a sufficiently high magnetic field,  $h > h_{c1}$ , gain elastic energy by adjusting their lattice to the field.<sup>8,10,13-15</sup> This magneto-elastic distortion can be rather well approximated by a sinusoidal form,  $\delta_r = \delta \cos(qr)$ , with  $q = \pi + 2\pi \langle S_{tot}^z / N \rangle$ .<sup>10,15,16</sup> With these two modulations of  $\delta_r$ , the magnetic field induced transition from the dimerized to the incommensurate phase is continuous for structurally dimerized chains, while it is first order for spin-Peierls chains, where a jump of  $K\delta^2/4$  occurs in the elastic energy.<sup>15</sup>

In this work, the spin excitation spectra in a magnetic field of these two systems are contrasted. Using exact diagonalization techniques on finite lattices of up to  $N = 24$  sites with periodic boundary conditions, the triplet and singlet excitations are calculated, allowing a direct comparison with inelastic neutron and Raman experiments. The strength of this method, although restricted to relatively small lattice sizes, is the accessibility of the full excitation spectrum for a given cluster. As our interest is primarily in the magnetic response, we concentrate on two effective,

purely magnetic model Hamiltonians,  $H_{dim}$  and  $H_{sP}$ , derived from  $H$  (Eq. 1). Phonon contributions, other than entering via the parametrization of  $\delta_r$  will be neglected.

For the structurally dimerized spin-1/2 antiferromagnetic Heisenberg chain, the model Hamiltonian  $H$  reduces to

$$H_{dim} = J \sum_{r=1}^N (1 + \delta(-1)^r) \mathbf{S}_r \cdot \mathbf{S}_{r+1}. \quad (2)$$

In a quasi-one-dimensional compound, such as  $KCuCl_3$ , the dimerization parameter,  $\delta > 0$ , originates from the alternating spacing of the spin-carrying  $Cu^{2+}$  ions.<sup>17</sup> In the limit  $\delta = 1$ , the system is an ensemble of  $N/2$  uncoupled dimers with only two energy levels per dimer, and a spin gap  $\Delta_z = 2J$ . In the opposite limit  $\delta = 0$ ,  $H_{dim}$  reduces to the isotropic antiferromagnetic Heisenberg chain which is quasi-long-range ordered, and thus belongs to a different universality class from the dimerized system. For sufficiently small lattice dimerizations, a regime with sizeable inter-dimer interactions can be identified with the scaling properties of the massive Thirring model.<sup>5</sup>

The effective magnetic Hamiltonian for spin-Peierls compounds is given by<sup>10</sup>

$$H_{sP} = J \sum_{r=1}^N (1 + \delta \cos(qr)) \mathbf{S}_r \cdot \mathbf{S}_{r+1}. \quad (3)$$

Here, the feedback due to the interactions of the spins with the lattice phonons enters through a field dependent modulation of the effective nearest-neighbor exchange integral,  $J_{eff}(r) = J(1 + \delta \cos(qr))$ , where  $q = \pi + 2\pi \langle S_{tot}^z / N \rangle$ . In the commensurate phase ( $h < h_{c1}$ ), the modulation is fixed at  $q = \pi$ , and  $H_{sP}$  is identical to  $H_{dim}$ . However, in the incommensurate regime  $q$  continuously grows from  $\pi$  to  $2\pi$ , mimicking the elastic distortion of the underlying lattice due to the dynamical coupling with the spins. Hence, all eigenstates of this system have a spin as well as a phonon component.<sup>18</sup>

In the subsequent section, the spin excitation spectra of structurally dimerized chains ( $H_{dim}$ ) in a magnetic field are discussed, followed by a section on spin-Peierls systems ( $H_{sP}$ ). We finish with some concluding remarks. As we are interested in capturing the generic features, and in particular the differences, of the two physical situations described above, no compound specific parameters, such as inter-chain or next nearest-neighbor exchange couplings, are considered. Rather, our focus will be on understanding the characteristic features of the phases in the most elementary magnetic models.

## II. STRUCTURALLY DIMERIZED CHAIN

It is remarkable that for some quasi-one-dimensional compounds, such as  $(VO)_2P_2O_7$  and  $CuGeO_3$ , it has been quite difficult to establish a unique microscopic model.<sup>1,19–21</sup> For example, from fits to early measurements of the uniform susceptibility on  $(VO)_2P_2O_7$  it has been concluded that this material is either a structurally dimerized or a frustrated spin-1/2 Heisenberg chain with a sizeable next-nearest-neighbor exchange coupling.<sup>19,21</sup> In both cases, a spin gap opens up either due to a structural or to a frustration induced dimerization, and the resulting thermodynamic response is quite similar for the two proposed models. Only recently, it could be shown by inelastic neutron scattering spectroscopy that  $(VO)_2P_2O_7$  is indeed a structurally dimerized chain, and that it is the lattice distortion rather than any frustration which gives rise to the observed spin gap.<sup>1</sup> Similarly, there are still rather different effective parameter sets for  $\delta$  and  $J_2$  used in the current literature on the spin-Peierls compound  $CuGeO_3$ . In one case ( $\delta = 0.03$ ,  $J_2 = 0.24$ ) the spin gap opens because of the lattice distortion<sup>20</sup>, while in the other case ( $\delta = 0.014$ ,  $J_2 = 0.36$ ) the frustration alone is large enough to cause a spin gap.<sup>22</sup> It is thus of particular interest to examine the full spin excitation spectrum of these quasi-one-dimensional materials in a magnetic field, in order to pinpoint the most relevant microscopic interactions.

Let us start by discussing the phase diagram of the structurally dimerized spin-1/2 Heisenberg chain in a magnetic field, shown in Fig. 1. (i) for  $|h| < h_{c1}$ , the system is in a spin-liquid phase with a singlet-triplet spin gap  $\Delta_z$  and  $h_{c1} = \Delta_z$ ; (ii) for  $h_{c1} < |h| < h_{c2}$  it is a gapless spin-density wave with a field-dependent modulation; and (iii) for  $|h| > h_{c2} = 2J$  it is fully spin-polarized in the direction of the applied magnetic field. To determine the dependence of  $\Delta_z$  on the dimerization, we use Shanks' transformation<sup>23,24</sup> on lattices of up to  $N=24$  sites. The asymptotic form of the spin gap for a given dimerization obeys a finite-size scaling relation,

$$\Delta_z(N, \delta) = \Delta_z(N = \infty, \delta) + A(\delta) \exp(-\Gamma(\delta)N), \quad (4)$$

where the constants  $A(\delta)$  and  $\Gamma(\delta)$  are obtained from Shanks' recursive equations<sup>23,24</sup>. In accordance with Ref.<sup>25</sup>, we find that the initially proposed dependence,  $\Delta_z(N = \infty, \delta) \propto \delta^{2/3} / \sqrt{|\log \delta|}$ ,<sup>7,26,27</sup> matches our extrapolation rather

poorly, while the form  $\Delta_z(N = \infty, \delta) = 2\delta^{3/4}$  (shown in Fig. 1) gives an excellent fit to our data over the whole range of parameter space,  $\delta \in (0, 1]$ . One likely reason for this discrepancy is that the initial analytical prediction is valid only for very small values of  $\delta$ , difficult to access with a finite-size scaling procedure. Furthermore, in this regime higher order logarithmic corrections also become important.<sup>28</sup> Down to rather small values of  $\delta$  ( $\delta > 0.3$ ), the dependence of the spin gap is linear to leading order,  $\Delta_z \approx (1 + 3\delta)/2$ , indicating that the picture of weakly interacting dimers - a perturbation about the limit of isolated dimers ( $\delta = 1$ ) - is applicable in this parameter regime. However, at low values of the dimerization parameter ( $\delta \lesssim 0.3$ ) the interactions between the dimers become increasingly important, leading to a deviation from the linear dependence of the spin gap on  $\delta$ .

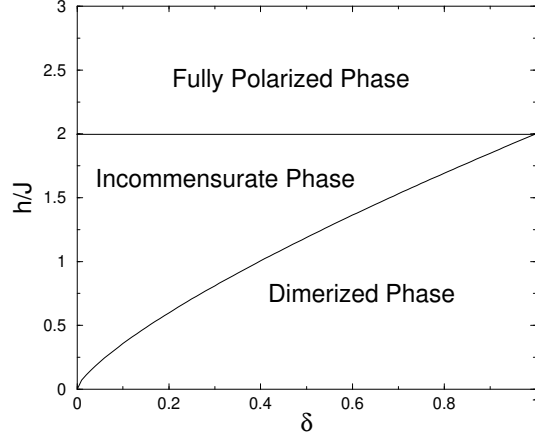


FIG. 1. Phase diagram of the structurally dimerized spin-1/2 Heisenberg chain in a magnetic field.  $\delta$  is the dimerization parameter.

The energy gaps between the groundstate and the lowest excited singlet and triplet as a function of the lattice dimerization are shown in Fig. 2. The magnitudes of the gaps in this figure quantitatively resemble the thermodynamic limit ( $N \rightarrow \infty$ ), as they were obtained from Shanks' transformation.<sup>29</sup> In the limit of vanishing dimerization, the gaps disappear, indicating that the groundstate is qualitatively different for the cases of vanishing and finite dimerization. The singlet gap is always larger than the triplet gap, and their ratio is  $\Delta_S/\Delta_z = 2$  for most of parameter space.<sup>30,31</sup> However, at lower values of  $\delta$  this ratio becomes smaller, possibly approaching the predicted value of  $\sqrt{3}$  as  $\delta \rightarrow 0$ .<sup>4,32</sup> Unfortunately, the quality of our finite size extrapolation procedure deteriorates in this limit, and no definite confirmation of  $\Delta_S/\Delta_z = \sqrt{3}$  can be drawn from this study, although our data is consistent with this value. It is clear, however, that the region of small dimerization must be governed by a field theory such as the massive Thirring model with a non-linear dependence of the excitation gaps on the effective mass, which in turn is proportional to  $\delta$ .<sup>5</sup>

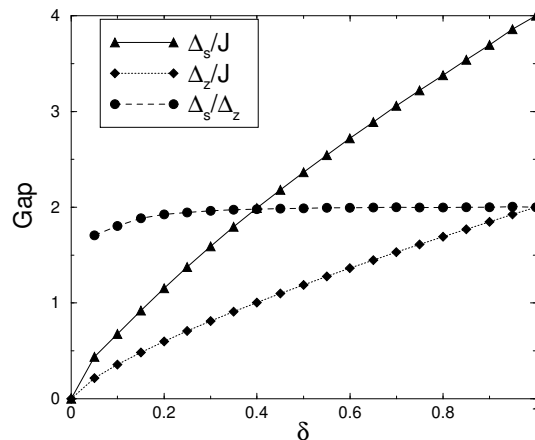


FIG. 2. Singlet and triplet spin gaps in the structurally dimerized spin-1/2 Heisenberg chain at zero magnetic field, obtained by Shanks' transformation on lattices of up to  $N=24$  sites. (i) diamonds: singlet-triplet gap, (ii) triangles: singlet-singlet gap, (iii) circles: ratio of singlet-singlet and singlet-triplet gap.

In Fig. 3, the triplet excitation spectra of the structurally dimerized spin-1/2 Heisenberg chain are shown, along with the corresponding dispersion relations in the insets. These spectra were calculated by an exact numerical diagonalization of 18-site chains with periodic boundary conditions, combined with a continued fraction expansion to obtain the full dynamical response functions. Let us first examine the dynamical spin structure factor,

$$S^{zz}(k, \omega) = \sum_n |\langle n | S_k^z | 0 \rangle|^2 \delta(\omega - E_n + E_0), \quad (5)$$

where  $S_k^z = \frac{1}{\sqrt{N}} \sum_r \exp(ikr) S_r^z$  is the projection of the spin operator parallel to the applied magnetic field,  $|n\rangle$  denotes an eigenstate of the Hamiltonian with energy  $E_n$ , orthogonal to the groundstate with energy  $E_0$ , and magnetization  $m = \langle S_{tot}^z / N \rangle \in [0, 1/2]$ . In the dimerized phase (Fig. 3(a)), the dominating feature in the spectrum is the one-magnon bound state with an onset frequency  $\omega = \Delta_z \approx (1 + 3\delta)/2$ , well separated from a continuum of states starting at twice this energy. Increasing the magnetic field, the one-magnon bound state moves down to lower energies, and eventually the gap closes at  $h = h_{c1}$  (Fig. 3(b)). Beyond  $h_{c1}$ , the soliton-antisoliton confinement potential is thus overcome by the magnetic field, and the bound state decays into a low-energy two-spinon continuum, similar to the spin-1/2 Heisenberg chain. In addition, there are continua of states at higher energies. In particular the lowest continuum (starting at  $\omega = \Delta_z$ ) carries most of the spectral weight. At the onset of the incommensurate phase ( $h = h_{c1}$ , Fig. 3(b)) the phase space of this low-energy continuum is strongly restricted, and therefore its width is small. The reason will become clear from the discussion below in terms of the corresponding spinless fermion picture. As the applied field is increased from  $h_{c1}$  to  $h_{c2}$ , the width of the low-energy continuum grows, and the wave vector of the dominant infrared divergence moves continuously from  $q = \pi$  to  $q = 2\pi$ . In Fig. 3(c), the triplet excitation spectra are shown at a particular magnetization,  $m = 4/18$ , corresponding to a magnetic field  $h \simeq 1.58J$ . Clearly, the modulation at this field is incommensurate, and the magnetic unit cell is enlarged by approximately a factor of two with respect to its size at zero field. Furthermore, the phase space for triplet excitations is reduced with increasing magnetic field, leading to an overall loss of spectral weight at higher fields. Finally, close to  $h_{c2}$  two triplet bands emerge, split by a dimerization gap,  $\Delta_{\pm} = 2\delta$  (Fig. 3(d)). Low-energy spectral weight away from long wavelengths disappears, and the low-frequency dispersion approaches  $\omega \propto k^2$ , characteristic for ferromagnetism.

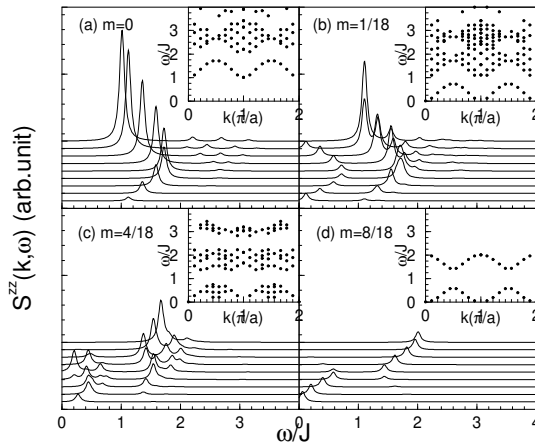


FIG. 3. Triplet excitation spectra of the structurally dimerized spin-1/2 Heisenberg chain in a magnetic field, calculated on an 18-site lattice with  $\delta = 0.4$ . The lowest curve is the dynamical spin structure factor at momentum transfer  $k = 0$ , and the highest at  $k = \pi$ . (a) Dimerized regime ( $h = 0$ ), (b) onset of incommensurate phase ( $h = h_{c1}$ ), (c) center of incommensurate phase ( $h_{c1} < h < h_{c2}$ ), (d) incommensurate phase at a high magnetic field, close to  $h_{c2}$ . The corresponding pole positions are shown in the insets.

The Hamiltonian of the structurally dimerized spin-1/2 Heisenberg chain can be mapped onto a model of spinless fermions via the Jordan-Wigner transformation. Due to the lattice dimerization, the spinless fermion band is split into two parts which disperse according to

$$\omega_{\pm}(k)/J = 1 \pm \sqrt{\delta^2 + (1 - \delta^2) \cos^2(k)}, \quad (6)$$

giving rise to a dimerization gap,  $\Delta_{\pm} = 2\delta$ , and to a total single particle bandwidth of  $2J$ . While these dispersion relations are exact in the XY-limit of  $H_{dim}$ , they are only slightly renormalized in the isotropic Heisenberg limit for

sufficiently large dimerization values ( $\delta > 0.3$ ), as can be seen by comparing  $\omega_-(k)$  and  $\omega_+(k)$  with the dispersions in the inset of Fig. 3(d). Furthermore, in the spinless fermion picture, the applied field corresponds to a chemical potential. At vanishing magnetic field, the chemical potential lies in the center of the gap between  $\omega_-$  and  $\omega_+$ . In order to excite an unbound pair of particles, a minimum energy of  $2\Delta_{\pm}$  is needed. In addition, due to the attractive scattering between the spinless fermions, an exciton-type particle-hole bound state is formed with a minimum energy of  $\Delta_z(h)$ , dispersing at  $h = 0$  as

$$\omega_z(k)/J = (1 + \delta) - (1 - \delta) \cos(2k)/2, \quad (7)$$

as observed in the inset of Fig. 3(a).<sup>4</sup> At small magnetic fields ( $h < h_{c1}$ ) this dominant one-magnon triplet mode carries most of the weight in the dynamical structure factor. Furthermore, there is a second gap ( $\Delta_2 = \Delta_z$ ) between the one-magnon bound state and a continuum of states which is a simple convolution of two magnons with a dispersion  $\omega_z(k)$ . With increasing magnetic field ( $h \rightarrow h_{c1}$ ) the bound state moves down to lower energies, and eventually  $\Delta_z$  vanishes at  $h_{c1}$ , whereas the onset of the continuum now occurs at  $\Delta_2(h = h_{c1}) = \Delta_z(h = 0)$ . Beyond  $h_{c1}$  the one-magnon bound state disappears and decays into a particle-hole continuum as the effective confining potential is overcome by the applied field.

Using only  $\omega_z(k)$  and  $\omega_{\pm}(k)$ , the complete magnetic field dependence of the triplet spectra can thus be understood qualitatively within a simple rigid-band picture. In the incommensurate phase, the chemical potential moves into the lower band,  $\omega_-(k)$ . The continuum of states at low energies arises from two-particle excitations within  $\omega_-(k)$ , whereas the continua at higher frequencies stem from processes involving interband scattering. The modulation wave vector  $q$ , corresponding to the applied magnetic field  $h$ , is obtained from the solution of  $h = \omega_-(q)$ . At fields slightly above  $h_{c1}$ , the phase space for intraband scattering processes are restricted within the lower band which is almost full. This is the reason for the narrow width of the low-energy continuum in Fig. 3(b), just at  $h = h_{c1}$ . At large magnetic fields,  $h \lesssim h_{c2}$ , the phase space of triplet excitations is exhausted, and the dynamical structure factor traces out the single particle bands of the spinless fermions (Fig. 3(d)).

Because the spectra in Fig. 3 were obtained on finite-size lattices, there are no true branch cuts in  $S^{zz}(k, \omega)$ . Rather, discrete sets of poles appear where continua are expected to emerge in the thermodynamic limit. In order to distinguish bound state poles from sets of poles which become part of a continuum in the thermodynamic limit, a finite-size scaling analysis of the individual pole positions and weights is necessary. From such an extrapolation, using chains with  $N = 4, \dots, 24$  sites, we find that the bound state with  $\omega_z(k)$  (Fig. 3(a)) is indeed stable, whereas the other poles in the spectrum merge into continua as the lattice size is increased to infinity. At smaller values of the lattice dimerization ( $\delta \lesssim 0.3$ ), the general features of the triplet spectra are the same as discussed above. However, once the bandwidths of  $\omega_{\pm}(k)$  become larger than the dimerization gap separating the two bands,  $\Delta_{\pm}$ , the higher-energy continua, which are separated from each other for larger dimerizations, begin to overlap. Using the exact dispersion expressions for the XY limit (Eq. 6), this crossover occurs at  $\delta_c = 1/3 \approx 0.3$ , consistent with the deviations from the weakly interacting dimer picture observed in our numerical data.

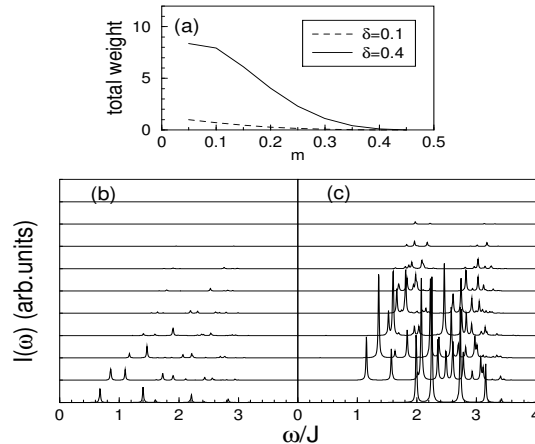


FIG. 4. Raman spectra for a 20-site spin-1/2 structurally dimerized Heisenberg chain in a magnetic field with (b)  $\delta = 0.1$  and (c)  $\delta = 0.4$ . The integrated weight for these two cases is shown in (a). The spectra are for magnetizations  $m = 0$  (lowest curve) up to  $m = 9/20$  (top curve).

Let us now turn to the spin excitation spectra of the structurally dimerized spin chain in a magnetic field, as they are probed by Raman scattering measurements. Within the Loudon-Fleury theory<sup>33</sup> - assuming resonant scattering

- the effective  $A_{1g}$  Raman operator of a one-dimensional spin system is proportional to  $\sum_r \mathbf{S}_r \cdot \mathbf{S}_{r+1}$ . Setting the proportionality constant equal to one, the dynamical Raman response function takes the form

$$I(\omega) = \sum_n |\langle n | \sum_r \mathbf{S}_r \cdot \mathbf{S}_{r+1} | 0 \rangle|^2 \delta(\omega - E_n + E_0). \quad (8)$$

In the following discussion of  $I(\omega)$ , terms in the Raman operator which are proportional to the Hamiltonian are omitted.<sup>34</sup> In Fig. 4 the Raman spectra for 20-site chains are shown as a function of the magnetic field. At zero magnetization ( $h < h_{c1}$ ), one singlet bound state is expected with a gap  $\Delta_s$ , followed by a continuum of excitations at higher energies, involving 4 spinons.<sup>32</sup> In the regime of large dimerization ( $\delta > \delta_c$ ), the singlet gap is at  $\Delta_s = 2\Delta_z \simeq (1 + 3\delta)J$  (Fig. 4(c)). This bound state is best understood by considering the limit of complete dimerization ( $\delta = 1$ ). The corresponding groundstate at  $h = 0$  is a product of singlet dimers with energy  $-3J/2$  per dimer.<sup>25</sup> Two such dimer singlets can be excited by the Raman operator into a 4-site singlet state. The energy difference,  $\Delta_s$ , between these states is approximately equal to  $(1 + 3\delta)J$  as long as the dimer-dimer interactions are sufficiently small ( $\delta > \delta_c$ ). In the limit of complete dimerization, one obtains exactly  $\Delta_s = 4J$ . In the opposite limit, the singlet bound state moves to lower energies (Fig. 4(b)), and most of the spectral weight is transferred into the zero-frequency peak, not shown here. Apart from the bound state at  $\Delta_s$ , there is a continuum of excitations at higher energies. Evidently, the spectra in Fig. 4 are plagued by severe finite-size effects, such that it is particularly difficult to distinguish by inspection the precursors of continua from emerging isolated bound states.<sup>35</sup> However, from the scaling behavior of the individual pole positions and weights we conclude that our data at zero magnetic field is consistent with the picture of an isolated bound state at  $\Delta_s$ , followed by a continuum of states above a threshold  $\omega \gtrsim \Delta_z$  in the thermodynamic limit. Beyond  $h_{c1}$ , the bound state disappears, and the onset frequency of the continuum increases from  $\Delta_z$  at  $h_{c1}$  up to  $2J$  close to  $h_{c2}$ . In Fig. 4(a) the integrated weight of the Raman spectrum,  $W = \int d\omega I(\omega)$ , is plotted as a function of the magnetization.  $W$  becomes very small as  $\delta \rightarrow 0$ . Furthermore, with increasing magnetic field,  $W(m)$  decreases more rapidly - with a purely concave shape - in the case of small dimerization (Fig. 4(b)). However, this subtle difference is most likely of little experimental relevance because important compound specific contributions, such as frustrating longer range interactions or interchain coupling, have been neglected in this discussion.

### III. SPIN-PEIERLS CHAIN

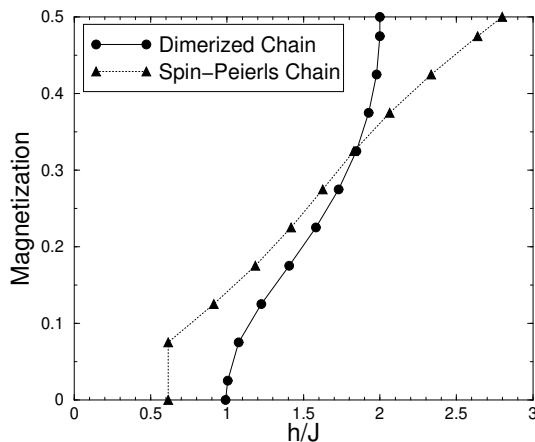


FIG. 5. Magnetization curves of the spin-1/2 structurally dimerized Heisenberg chain (circles) and of the spin-Peierls chain (triangles) with  $\delta = 0.4$ . At  $h_{c1}$ , the magnetization of the spin-Peierls system jumps discontinuously from zero to a finite value, indicating a first order transition, whereas in the structurally dimerized chain the transition into the incommensurate regime is continuous.

In contrast to the structurally dimerized chains, spin-Peierls chains have a gapped incommensurate phase as their lattice distortion adapts magneto-elastically to the applied field. For a self-consistent treatment of this incommensurate regime, the phonon and the spin degrees of freedom have thus to be treated on an equal footing. In large scale numerical studies of the full adiabatic spin-phonon Hamiltonian  $H$  (Eq. 1), it has been shown that the structural distortion of the lattice and the modulation of the local magnetization have the shape of solitons, natural for one-dimensional

systems.<sup>15,12</sup> As the focus of this work is the magnetic response, an effective parametrization for the lattice distortion of the form  $\delta_r = \delta \cos(qr)$  is used,<sup>10</sup> instead of treating the elastic part of  $H$  self-consistently. Especially at higher magnetic fields, this form gives results almost identical to the self-consistent treatment of the lattice dynamics for observables such as the local magnetization. Furthermore, we have verified that other (solitonic) parametrizations<sup>16</sup> yield spin excitation spectra which are only minutely different to those with a sinusoidal lattice distortion.

In Fig. 5, the magnetization curves,  $m(h)$ , of the spin-1/2 structurally dimerized Heisenberg chain and of the spin-Peierls system are shown. They were calculated by numerical diagonalization of 22-site chains. The magnetization of the structurally dimerized chain has a plateau between  $h = 0$  and  $h_{c1} = \Delta_z$ .  $m(h)$  then rises continuously from zero at  $h_{c1}$  up to  $m = 1/2$  at  $h_{c2} = 2J$ . The particle-hole symmetry of the corresponding spinless fermion band is reflected by the point symmetry of  $m(h)$  about its midpoint. In contrast, the magnetization of the spin-Peierls chain jumps discontinuously at  $h_{c1}$  from zero to a finite value. The position of  $h_{c1}$  and the magnitude of the discontinuity depend on the lattice spring constant  $K$ . Therefore, a precise determination of these quantities is beyond the realm of our effective - purely magnetic - theory using  $H_{sP}$ . However, from self-consistent calculations it has been concluded that the second order transition line,  $h_{c1}(\delta)$ , for the structurally dimerized chain (Fig. 1) becomes first order in the spin-Peierls case, and moves down towards lower fields with increasing lattice spring constant.<sup>8,15,36</sup>

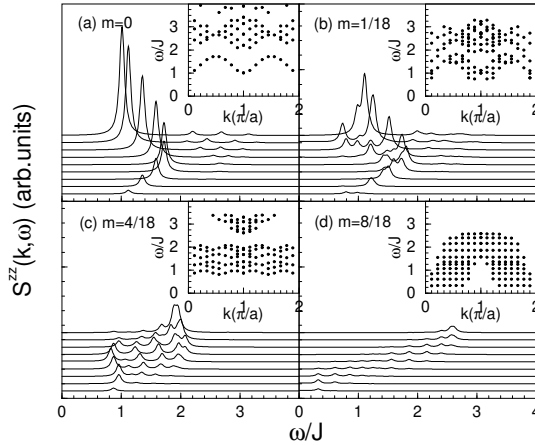


FIG. 6. Triplet excitation spectra of the spin-1/2 spin-Peierls chain in a magnetic field, calculated on an 18-site lattice with  $\delta = 0.4$ . The lowest curve is the dynamical spin structure factor at momentum transfer  $k = 0$ , and the highest at  $k = \pi$ . (a) Dimerized regime ( $h = 0$ ), (b) onset of incommensurate phase ( $h = h_{c1}$ ), (c) center of incommensurate phase ( $h_{c1} < h < h_{c2}$ ), (d) incommensurate phase at a high magnetic field, close to  $h_{c2}$ . The corresponding pole positions are shown in the insets.

Let us now turn to the triplet excitation spectrum of the spin-Peierls chain in a magnetic field, shown in Fig. 6. For  $h < h_{c1}$ , the spin response is identical to that of the structurally dimerized chain (Fig. 6(a)). The lattice dimerization gives rise to a scattering potential peaked at  $q = 2k_F = \pi$ . This attraction between pairs of particles at opposite ends of the Brillouin zone leads to the formation of a one-magnon bound state. In the incommensurate phase (Fig. 6(b-d)), the lattice distortion,  $q = \pi + 2\pi m(h)$ , adapts to the magnetic field, thus supporting a bound state with a minimum energy  $\omega = \Delta_z(h) \neq \Delta_z(h = 0)$  and a modulation  $q$  due to an effective field dependent potential,  $V_{eff}(q) \sim \delta \cos(qr)$ . At higher energies, there are continua of states. In contrast to the dimerized phase, in the incommensurate regime the second gap, between the onset of the bound state and the onset of the lowest continuum, is smaller than  $\Delta_z(h)$ . This can be understood within the spinless fermion picture: as the magnetic field is increased beyond  $h_{c1}$ , the corresponding Fermi wave vector moves away from  $\pi/2$ . Opposite to the case of the structurally dimerized chain, the scattering potential adapts to the changing magnetic field, such that there is always an instability at the Fermi level due to particle-hole scattering with momentum transfer  $q = 2k_F(h) = \pi + 2\pi m(h)$ . Furthermore, in the incommensurate phase the chemical potential is offset from the center of the gap. The energy difference between  $\mu$  and the lower edge of the gap is  $\Delta_-(h)$ , and between  $\mu$  and the upper edge it is  $\Delta_+(h)$ , shown in Fig. 7, where the values of  $\Delta_-$  and  $\Delta_+$  have been evaluated by acting with  $S^-$  and  $S^+$  on the groundstate.<sup>10</sup> The onset of the one-magnon bound state occurs at a higher energy,  $\Delta_z(h) > (\Delta_-(h) + \Delta_+(h))/2$ . Only in the dimerized phase, it is found that  $\Delta_z = \Delta_- = \Delta_+$ , and thus  $\Delta_z = (\Delta_- + \Delta_+)/2$  because of the additional particle-hole symmetry for the special case of half-filling. The magnetic field dependence of the triplet spectra in Fig. 6 follows exactly this picture. For example, at magnetization  $m = 4/18$  (Fig. 6(c)), the onset of the one-magnon bound state is at  $\omega = 0.82J$ , whereas the lowest continuum of states starts at  $\Delta_- + \Delta_+ = 0.39J + 0.69J = 1.08J$ , thus separating the bound state from the continuum by a second gap of  $\Delta_2 = 0.26J < \Delta_z(h) = 0.82J$ .

Similar to the structurally dimerized chain, the phase space of triplet excitations is gradually reduced in the incommensurate phase of the spin-Peierls system, leading to a loss of spectral weight in  $S^{zz}(k, \omega)$  with increasing magnetic field. Furthermore, the widths of the triplet bands shrink at higher fields, indicating an effective localization of triplets. For example, the band width  $W$  of the one-magnon bound state is drastically reduced (see inset of Fig. 7), going practically to zero beyond  $m_c \approx 0.3$ . Its dispersion,  $\omega_z(k)$ , oscillates rapidly as the modulation vector  $q$  approaches  $2\pi$ . The reason for this behavior is that the real-space magnetic unit cell grows with increasing magnetic field. At sufficiently high fields, it grows beyond the size of any finite cluster. For the parameter choice and lattice size we use, this happens at approximately  $m_c$ . Beyond  $m_c$ , the corresponding modulation of the effective nearest-neighbor exchange integral,  $J_{eff}(r) = J(1 + \delta \cos(qr))$ , has only one minimum in the finite chain where triplets are trapped, leading to a “smearing” of  $\omega(k)$  in momentum space (Fig. 6(d)). While this localization of magnons is obviously an artefact of the finite cluster calculation, it may be realized in mesoscopic chains, as soon as the size of the magnetic unit cell exceeds the mesoscopic length scale. Also, such a localization can easily be stabilized by a pinning of the distortion, to which a physical system is highly susceptible as the modulation grows toward infinity. In this case, a real-space picture of (almost) localized triplets is most appropriate at high magnetic fields, close to  $h_{c2}$ .

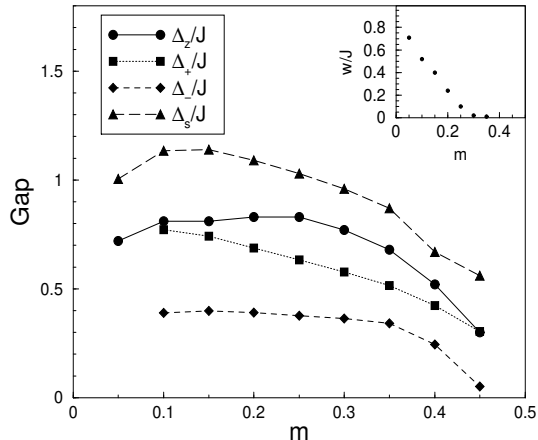


FIG. 7. Singlet and triplet gaps in the incommensurate phase of the spin-Peierls chain with  $\delta = 0.4$ , calculated on a 20-site lattice. (i) circles: triplet gap parallel to the applied field, (ii) squares and diamonds: triplet gaps perpendicular to the applied field, (iii) triangles: singlet gap.

The singlet gap  $\Delta_s$ , shown in Fig. 7, corresponds to the onset of the finite frequency Raman spectrum (Fig. 8). It is always larger than the triplet gap, and has a similar dependence on the magnetization. From an examination of the finite-size scaling behavior of the poles in the Raman spectrum, there appears to be a low-energy singlet bound state for all fields  $h < h_{c2}$ .<sup>4,32</sup> In particular, an analysis of the  $\delta = 0.4$  Raman spectra (Fig. 8(c)) suggests that in the thermodynamic limit the two lowest poles merge into one, and their spectral weight extrapolates to a finite value, thus indicating the existence of a two-magnon bound state. For smaller dimerizations (such as  $\delta = 0.1$  in Fig. 8(b)) it is difficult to determine from our finite-size data whether there is a bound state. This is consistent with a recent numerical study of the Raman spectrum in  $CuGeO_3$  which has considered an even smaller dimerization constant  $\delta \simeq 0.03$ .<sup>30</sup> Here it was argued that the strong magnon-magnon interactions destabilize the singlet bound state. However, as seen in Figs. 8(b) and (c), the Raman excitation spectra are qualitatively rather similar for these two parameter choices. Consider for example the spectra at the onset of the incommensurate phase ( $m = 1/20$ ), shown in the second lowest curves of Figs. 8(b) and (c). At low energies, there is a pair of poles (the second pole is not visible for  $\delta = 0.1$ ), separated from a set of poles at higher energies with a close spacing. As discussed above, the low-frequency poles merge in the thermodynamic limit, whereas the high-frequency set of poles appears to evolve into a continuum of states. We therefore suspect that singlet bound states may exist at the lower edge of the spectrum for any finite  $\delta$ , but much larger clusters may be needed for a numerical confirmation of the singlet bound state at small values of  $\delta$ . Furthermore, the total finite-frequency spectral weight  $W(m)$ , shown in Fig. 8(a), has the same dependence on the magnetization for both choices of  $\delta$ , indicating that there should be only one massive field theory applicable for the whole range  $\delta \in (0, 1]$ .



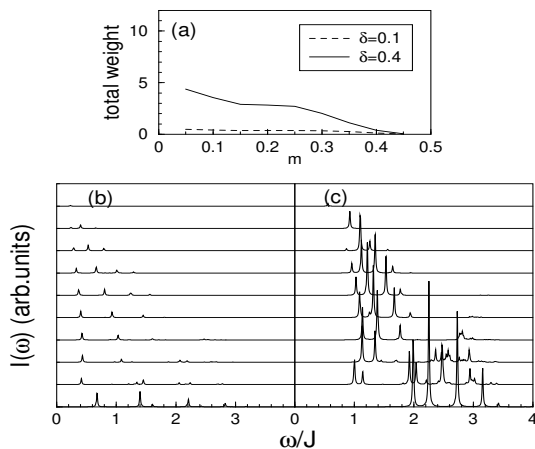


FIG. 8. Raman spectra for a 20-site spin-Peierls chain in a magnetic field with (b)  $\delta = 0.1$  and (c)  $\delta = 0.4$ . The integrated weight for these two cases is shown in (a). The spectra are for magnetizations  $m = 0$  (lowest curve) up to  $m = 9/20$  (top curve).

#### IV. CONCLUSIONS

In summary, we have analyzed the spin excitation spectra for two distinct models in a magnetic field: the structurally dimerized chain and the spin-Peierls chain. Below a critical field,  $h_{c1}$ , both systems are in a spin liquid phase, composed of interacting singlet dimers. Above  $h_{c1}$ , the spin gap of the structurally dimerized chain closes, whereas the spin-Peierls system supports a singlet-triplet gap up to  $h_{c2}$ . Therefore, the excitation spectra of these two models are quite different in their incommensurate phases. In the structurally dimerized chain, a soliton-antisoliton continuum appears at low energies, separated by a dimerization gap  $\Delta_{\pm} = 2\delta$  from a second continuum at higher frequencies. In the spin-Peierls chain there is a triplet bound state with an onset at  $\Delta_z$ , and a higher-energy continuum of states, starting at  $\Delta_- + \Delta_+ < 2\Delta_z$ . Parts of the triplet band may thus overlap with the continuum. Common features in the spin excitation spectra of these two systems are (i) an incommensurate, field-dependent modulation  $q = \pi + 2\pi m(h)$  for  $h_{c1} < h < h_{c2}$ , (ii) a loss of overall spectral weight with increasing magnetic field, and (iii) full spin polarization beyond  $h_{c2}$ .

Furthermore, there are qualitative changes in the spectra of the structurally dimerized chain, depending on the magnitude of the dimerization parameter  $\delta$ . The region of large dimerization in the  $h - \delta$  phase diagram can be understood within the valence bond picture of weakly interacting dimers, whereas for small values of  $\delta$  the interactions between the dimers are important, reducing the ratio of the singlet to the triplet gap and increasing the bandwidths of the spectral features.

The triplet excitation spectra of the spin-Peierls chain in the incommensurate phase contain a one-magnon bound state with an onset at  $\Delta_z$ , and a soliton-antisoliton continuum with an onset at higher frequencies,  $\omega = \Delta_- + \Delta_+$ . The actual dimerization strengths of real spin-Peierls compounds are typically smaller than the values we have studied here, which were chosen to improve numerical stability. However, the spin excitation spectra obtained for  $H_{sP}$  are qualitatively similar for the whole range of  $\delta$  we were able to study.

We wish to thank A. Honecker, B. Normand, G. Uhrig, and S. Wessel for useful discussions, and acknowledge the Zumbege Foundation for financial support.

<sup>1</sup> A.W. Garrett *et al.*, Phys. Rev. Lett. **79**, 745 (1997); D.A. Tennant *et al.*, Phys. Rev. Lett. **78**, 4998 (1997).

<sup>2</sup> M. Arai *et al.*, Phys. Rev. Lett. **77**, 3649 (1996).

<sup>3</sup> O. Fujita, J. Akimitsu, M. Nishi, and K. Kakurai, Phys. Rev. Lett. **74**, 1677 (1995).

<sup>4</sup> G.S. Uhrig and H.J. Schulz, Phys. Rev. B **54**, R9624 (1996); Phys. Rev. B **58**, 2900 (1998).

<sup>5</sup> I. Affleck in *Dynamical Properties of Unconventional Magnetic Systems*, edited by A.T. Skjeltorp and D. Sherrington (Kluwer Academic Publishers, 1997).

- <sup>6</sup> G.S. Uhrig, F. Schönfeld, M. Laukamp, and E. Dagotto, *Eur. Phys. J. B* **7**, 67 (1999).
- <sup>7</sup> M.C. Cross and D.S. Fisher, *Phys. Rev. B* **19**, 402 (1979).
- <sup>8</sup> R.A.T. de Lima and C. Tsallis, *Phys. Rev. B* **27**, 6896 (1983).
- <sup>9</sup> D. Khomskii, W. Geertsma, and M. Mostovoy, cond-mat/9609244.
- <sup>10</sup> G.S. Uhrig, F. Schönfeld, and J.P. Boucher, *Europhys. Lett.* **41** (4), 431 (1998); G.S. Uhrig in *Advances in Solid State Physics* 39, 291 (1999), edited by B. Kramer (Vieweg, Braunschweig).
- <sup>11</sup> G. Spronken, B. Fourcade, and Y. Lépine, *Phys. Rev. B* **33**, 1886 (1986).
- <sup>12</sup> A.E. Feiguin, J.A. Riera, A. Dobry, and H.A. Ceccatto, *Phys. Rev. B* **56**, 14607 (1997).
- <sup>13</sup> J.W. Bray *et al.*, in *Extended Linear Chain Compounds*, edited by J.S. Miller, (Plenum Press, New York, 1983), Vol. 3.
- <sup>14</sup> V. Kiryukhin, B. Keimer, J.P. Hill, and A. Vigliante, *Phys. Rev. Lett.* **76**, 4608 (1996).
- <sup>15</sup> F. Schönfeld, G. Bouzerar, G.S. Uhrig, and E. Müller-Hartmann, *Eur. Phys. J. B.* **5**, 521 (1998).
- <sup>16</sup> We have assumed for convenience that the lattice modulation is approximately sinusoidal. This is in good qualitative agreement with calculations which treat the lattice dynamics in a self-consistent way. However, it should be noted that the actual modulation has a solitonic form,  $\delta_r = \delta(-1)^r \tanh((r - r_0 - d/2)/\chi) \tanh((r - r_0 + d/2)/\chi)$ , where  $r_0$  denotes the position(s) of the largest local magnetization,  $\chi \sim v_s/\Delta_z$  is the soliton width, and  $d$  is the soliton-soliton distance. We have checked that this form gives results very similar to the sinusoidal form, which has been used throughout this paper.
- <sup>17</sup> N. Cavadini *et al.*, *Eur. Phys. J. B* **7**, 519 (1999). In this reference it has been proposed that this material might not have purely one-dimensional magnetic properties. However, there is a dominant direction with strong exchange couplings.
- <sup>18</sup> G. Uhrig, *Phys. Rev. B* **57**, R14004 (1998). In this paper a mapping is performed from the general spin-phonon Hamiltonian onto an effective adiabatic spin model, which we have adapted in this manuscript.
- <sup>19</sup> D.C. Johnston, J.W. Johnson, D.P. Goshorn, and A.J. Jacobson, *Phys. Rev. B* **35**, 219 (1987).
- <sup>20</sup> G. Castilla, S. Chakravarty, and V.J. Emery, *Phys. Rev. Lett* **75**, 1823 (1995).
- <sup>21</sup> T. Barnes and J. Riera, *Phys. Rev. B* **50**, 6817 (1994).
- <sup>22</sup> J. Riera and A. Dobry, *Phys. Rev. B* **51**, 16098 (1995).
- <sup>23</sup> D. Shanks, *J. Math. Phys.* **34**, 1 (1955).
- <sup>24</sup> T. Sakai and M. Takahashi, *Phys. Rev. B* **42**, 1090 (1990).
- <sup>25</sup> T. Barnes, J. Riera, and D.A. Tennant, *Phys. Rev. B* **59**, 11384 (1999).
- <sup>26</sup> J.L. Black and V.J. Emery, *Phys. Rev. B* **23**, 429 (1981).
- <sup>27</sup> A. Klümper, *Euro. Phys. J. B* **5**, 677 (1998).
- <sup>28</sup> I. Affleck, D. Gepner, H. J. Schulz, and T. Ziman, *J. Phys. A: Math. Gen.* **22**, 511 (1989).
- <sup>29</sup> The individual gaps of the finite-size clusters actually increase as  $\delta \rightarrow 0$ . However, a finite-size scaling analysis shows that in the thermodynamic limit the spin gap decreases monotonously as  $\delta$  is lowered from 1 to 0.
- <sup>30</sup> C. Gros *et al.*, *Phys. Rev. B* **55**, 15048 (1997).
- <sup>31</sup> G. Bouzerar, A.P. Kampf, and G.I. Japaridze, *Phys. Rev. B* **58**, 3120 (1998).
- <sup>32</sup> D. Augier, E. Sorenson, J. Riera, and D. Poilblanc, *Phys. Rev. B* **60**, 1075 (1999); E. Sorensen, I. Affleck, D. Augier, and D. Poilblanc, *Phys. Rev. B* **58**, R14701 (1998); D. Augier, D. Poilblanc, E. Sorenson, and I. Affleck, *Phys. Rev. B* **58**, 9110 (1998).
- <sup>33</sup> P.A. Fleury and R. Loudon, *Phys. Rev.* **166**, 514 (1968). The Raman operator may also contain alternating contributions, similar to the  $\delta$ -term in the Hamiltonian. We have verified that the inclusion of such a contribution modifies our results (Fig. 4) only slightly. For the sake of simplicity, we therefore stick with the easiest possible Raman operator in this paper.
- <sup>34</sup> Terms in the Raman operator which commute with the Hamiltonian contribute to a featureless peak at zero frequency. In the limit  $\delta = 0$ , the full spin Hamiltonian is proportional to the Raman operator, leading to a trivial Raman response:  $I(\omega) = \delta(\omega)$ . Here we are interested in the non-trivial features of  $I(\omega)$  away from  $\omega = 0$  at finite  $\delta$ .
- <sup>35</sup> Typically, a set of poles with decreasing weights for the higher-energy poles is indicative of an emerging continuum. This is the case for the three major poles at higher energies in the Raman spectra at zero field, whereas the lowest pole becomes an isolated bound state as  $N \rightarrow \infty$ .
- <sup>36</sup> R.J. Bursill, R.H. McKenzie, and C.J. Hamer, *Phys. Rev. Lett.* **83**, 408 (1999).